Biological Psychology 210 (2026) 109278

Contents lists available at ScienceDirect

Biological Psychology

journal homepage: www.elsevier.com/locate/biopsycho

Cardiac dynamics during social evaluative feedback: Evidence from intersubject representational similarity analysis

Jinhee Kim, Meeseung Lee, Daon Lee, Minyoung Kim, Hackjin Kim *

School of Psychology, Korea University, Republic of Korea

ARTICLE INFO

Keywords:
Social feedback
Behavioral bias
Intersubject representational similarity analysis
Cardiac deceleration
Heart rate variability

ABSTRACT

In everyday interactions, social evaluative feedback can elicit defensive responses that vary across individuals, underscoring the need to clarify the psychophysiological mechanisms underlying this variability. This study examined the cardiac correlates of defensive responses to social feedback, focusing on how cardiac activity reflects individual differences in self-protective behavior. Participants completed a mobile-based reciprocal artwork evaluation task while cardiac activity was continuously monitored via photoplethysmography using a wearable smartwatch. During the task, participants received positive, negative, or neutral feedback from partners and subsequently evaluated the creativity of the partner's artwork, indexing defensive behavioral responses. Feedback-evoked heart rate responses were analyzed using temporal intersubject representational similarity analysis (IS-RSA) to assess how dynamic cardiac similarity patterns related to individual differences in behavioral tendencies across feedback conditions. Results revealed that social feedback systematically influenced subsequent evaluations of the partner's artwork. Negative feedback elicited transient heart rate deceleration, whose magnitude was inversely associated with resting heart rate variability. IS-RSA further revealed that individuals who made more favorable judgments following positive feedback exhibited greater intersubject cardiac similarity during the early post-feedback period. Follow-up group analyses indicated that this convergence reflected transient heart rate deceleration among individuals with stronger behavioral bias. Together, these findings elucidate the physiological basis of self-protective bias in social contexts and highlight the role of individual psychophysiological variability.

1. Introduction

In everyday interactions, individuals frequently encounter social feedback ranging from praise to criticism. Negative social evaluations, in particular, can threaten self-esteem and elicit defensive responses aimed at protecting the self (Rodman et al., 2017; Yoon et al., 2018). These defensive reactions are expressed both psychologically and physiologically, including changes in heart rate (HR), skin conductance, and respiration (Noordewier et al., 2020; Roelofs et al., 2010). Understanding such psychophysiological responses is essential for elucidating the mechanisms that support emotional well-being and regulate interpersonal relationships.

Cardiovascular responses have long been used as informative physiological correlates of emotional processes (Candia-Rivera et al., 2022). HR dynamically adjusts to environmental demands through sympathetic and parasympathetic modulation of the autonomic nervous system, resulting in HR acceleration or deceleration. A well-established parasympathetically mediated response is phasic HR deceleration (Campbell et al., 2013), commonly observed following exposure to emotionally salient or threatening stimuli (Bradley et al., 2001; Klorman et al., 1977). This deceleration, thought to reflect vagal activation, is associated with enhanced attentional engagement and facilitates information gathering from the environment (Lacey, 1967; Porges & Raskin, 1969). Similar transient HR deceleration has been reported in evaluative feedback contexts, reflecting the temporal dynamics of feedback processing (Crone et al., 2003). A series of studies using a social judgment paradigm, in which participants predict whether an unfamiliar peer would like or dislike them, have consistently demonstrated that unexpected social rejection is associated with parasympathetically mediated cardiac slowing (Dekkers et al., 2015; Gunther Moor et al., 2010; Van der Veen et al., 2014; van der Veen et al., 2016). The findings suggest that HR deceleration is a reliable psychophysiological marker of social-evaluative threat. Moreover, autonomic responses to feedback vary across social contexts, indicating sensitivity not only to feedback

* Correspondence to: School of Psychology, Korea University, University Law Building, 145 Anam-ro, Seongbuk-gu, Seoul 02841, Republic of Korea.
E-mail address: hackjinkim@korea.ac.kr (H. Kim).

https://doi.org/10.1016/j.biopsycho.2026.109278
Received 23 January 2026; Received in revised form 12 April 2026; Accepted 29 April 2026
Available online 1 May 2026

valence but also to broader evaluative circumstances (Boukarras et al., 2022). Recent theoretical accounts further suggest that these cardiovascular dynamics reflect integrated brain–body states linking mental and physical health, underscoring their relevance for understanding adaptive and maladaptive processes in social contexts (Villringer et al., 2025).

Moreover, traditional analyses of HR responses often rely on univariate methods, such as averaging responses within fixed time windows or correlating mean physiological values with behavioral or self-report measures (Osumi & Ohira, 2016; van der Veen et al., 2016). Although informative, these approaches are limited in their ability to capture the complex and individualized physiological patterns underlying self-protective behavior. Furthermore, whether HR responses to social-evaluative feedback are systematically linked to individual differences in self-protective behavior has remained unexamined. To address these limitations, we employed a multivariate approach based on second-order statistics, comparing the geometrical structure of physiological data with that of behavioral data. Intersubject representational similarity analysis (IS-RSA) provides a powerful framework for assessing whether individuals with closely similar behavioral tendencies also exhibit strongly similar patterns of neural or physiological activity (Finn et al., 2020; Nguyen et al., 2019). While IS-RSA has been widely applied in fMRI and EEG studies of individual differences (Chen et al., 2017), its application to cardiac data remains relatively rare (Triana et al., 2024; Wang et al., 2022). Rather than focusing on mean HR values, IS-RSA quantifies how patterns of HR similarity across individuals correspond to patterns of behavioral similarity. For example, Wang et al. (2022) applied IS-RSA to HR variability (HRV) features derived from 20-second segments of negative-emotion virtual reality viewing, linking intersubject cardiac similarity to sociability traits. Moreover, dynamic implementations of IS-RSA using sliding-window approaches have been applied in EEG research to capture time-resolved patterns of interindividual similarity (Xu et al., 2023; Zhang et al., 2025). In the present study, we extend this dynamic IS-RSA framework to HR time series, enabling examination of temporally evolving physiological similarity.

While laboratory studies have yielded valuable insights, there is a growing need to extend this research beyond controlled settings. Smartphone-based tasks are increasingly used to assess cognitive and behavioral performance, enabling accessible and repeated measurements in naturalistic contexts (Moore et al., 2017). Simultaneously, consumer-grade wearable technologies allow continuous, unobtrusive physiological recording, offering new opportunities to study cardiovascular responses outside traditional laboratory environments (Stieger et al., 2018; Tutunji et al., 2023). Among these measures, HR derived from photoplethysmography (PPG) is widely used due to its minimal invasiveness and high participant acceptability. However, the reliability and validity of PPG-based HR measurements remain critical methodological considerations. Accordingly, the present study adopts an intermediate approach by acquiring PPG data from a consumer-grade wearable while participants performed a smartphone-based task in a controlled experimental setting and by examining how these measurements converge with cardiovascular responses obtained from research-grade physiological recordings.

The present study aimed to identify physiological signatures of social evaluative threat associated with self-protective behavior and to examine individual differences in behavioral and physiological response patterns. To our knowledge, this was the first study to apply intersubject representational similarity analysis to cardiac time-series data using wearable smartwatch-based measurements to examine how social evaluative feedback shapes individual differences in self-protective behavior and HR dynamics.

2. Methods

2.1. Participants

A total of 132 participants (mean age = 23.58 ± 2.71 years; 75 females, 57 males) were recruited at Korea University, through online advertisements. Inclusion criteria required participants to be adults (≥19 years), right-handed, with normal or corrected-to-normal vision, and without a self-reported history of neurological or psychiatric disorders. The study was approved by the Korea University Institutional Review Board, and all participants provided written informed consent prior to participation. Participants received KRW 48,000 as compensation.

In total, 3 participants were excluded from behavioral analyses: 1 consistently mirrored received feedback (e.g., 100% "creative" responses following positive/neutral feedback and 100% "not creative" responses following negative feedback), rendering the data uninformative for the intended evaluative process; 1 showed an unreliable model estimate (>8 standard deviation [SD] for β_{VSP}) due to near-uniform button presses; and 1 was excluded due to cardiac irregularities characterized by repeated segments with missing R-peaks in the ECG signal. This resulted in a final behavioral sample of 129 participants. For event-related HR analyses during the main behavioral task, an additional 26 participants were excluded due to physiological data transfer errors (n = 4) or motion-induced PPG artifacts (n = 22), defined as cases in which HR could not be reliably estimated in more than 20% of trials. The final physiological sample therefore comprised 103 participants. Participant demographic, physiological, lifestyle, and questionnaire characteristics are summarized in Table 1.

Power analysis was conducted to determine the required sample size. Effect size estimates were informed by prior studies examining cardiac responses to social evaluative feedback (e.g., being liked or disliked by others), which reported partial η^2 values ranging from .106 to .320 (Dekkers et al., 2015; Gunther Moor et al., 2010; Van der Veen et al., 2014), corresponding to Cohen's f = 0.34–0.69. Using G*Power 3.1.9.7 with α = .05, power = 0.80, and a conservative medium effect size of f = 0.25, the recommended sample size was 48 participants. The final sample (n = 103) therefore provided sufficient statistical basis to detect feedback-related differences in HR deceleration. For the association between HR deceleration and HRV index, the observed effect (r = −.307, n = 103) corresponded to an estimated power of approximately 0.80 (α = .05, two-tailed), implying that the sample size was sufficient for detecting effects of this magnitude.

Table 1
Participant characteristics.

	Total (n = 103)
Gender	47 Male, 56 Female
Age, years (mean, SD)	23.17 (2.52)
BMI	22.15 (3.24)
Resting heart rate (bpm)	80.67 (10.73)
HRV (RMSSD, ms)	34.28 (19.09)
Hours of sleep previous night	6.61 (1.33)
Alcohol consumption (days/week)	0.80 (0.95)
Physical activity (days/week)	2.29 (1.59)
PHQ-9	4.08 (4.28)
BFNE-II	37.76 (9.63)
RSES	31.52 (5.28)
SESS	68.34 (13.13)

Values are means (SD). Abbreviations: BMI, body mass index; HRV, heart rate variability; RMSSD, root mean square of successive differences; PHQ-9, Patient Health Questionnaire–9; BFNE-II, Brief Fear of Negative Evaluation Scale II; RSES, Rosenberg Self-Esteem Scale; SSES, State Self-Esteem Scale. Physical activity was indexed as the number of days per week participants engaged in at least 20 min of moderate-intensity activity during the past month (0–7 days). Alcohol consumption was indexed as the number of days per week participants reported drinking alcohol.

2.2. Apparatus

All experimental tasks were conducted in a sound-attenuated laboratory environment. Participants wore smartwatches (Samsung Galaxy Watch 4 or 6; Samsung Electronics, Suwon, Republic of Korea) on the left wrist. Cardiac signals were acquired using wearable electrocardiography (ECG; 500 Hz) and PPG (100 Hz). HRV was assessed using ECG when participants placed a finger on the watch's metal ring. During the artwork evaluation task, continuous ECG recording was not feasible due to manual smartphone responses; therefore, cardiac activity was continuously monitored using the PPG sensor.

All experiments were administered via a custom Android smartphone application installed on Samsung Galaxy A30 or A32 devices (Samsung Electronics, Suwon, Republic of Korea). The application presented stimuli, recorded behavioral responses, and communicated with the Galaxy Watch via Bluetooth to control sensor acquisition. Timestamps for stimulus onset, responses, and physiological signals were synchronized using the smartphone's internal clock to ensure temporal alignment. Physiological data were stored locally and automatically uploaded via encrypted transmission to a secure Microsoft Azure cloud server after each task.

2.3. Study procedure

Participants completed a previsit artwork creation task approximately 6 days before the laboratory session to strengthen the belief that sufficient time had elapsed for their work to be evaluated by others. In this web-based task, participants created and titled artworks using a customized digital sketchpad (Sketch.io, Portland, OR, USA) featuring a pencil tool and selectable clipping images (e.g., fruits, vegetables, snacks, and office supplies). Participants were informed that their artwork and titles would be evaluated for creativity by other participants and used in a subsequent laboratory task.

Participants attended two sessions spaced approximately 1–2 days apart. Data analyzed in the present study were obtained from the first session, which included baseline HRV recording and the artwork evaluation task, and from questionnaire measures collected during the second session. Additional tasks, including heartbeat counting and social comparison tasks, were not included in the current analyses.

2.3.1. Baseline heart rate variability

Baseline HRV was recorded for six minutes using the Galaxy Watch ECG sensor. Participants remained seated and motionless, with their right index finger placed on the sensor throughout the recording to ensure continuous signal acquisition. Following completion, data quality was inspected to confirm uninterrupted contact and signal integrity.

2.3.2. Reciprocal artwork evaluation task

Participants completed a reciprocal artwork evaluation task adapted from our previous study (Yoon et al., 2018). The task comprised 75 trials, in which each participant received ostensible feedback on the creativity of their artwork from 75 partners. Feedback was presented in three valence conditions: positive ("creative," 30 trials; lit bulb with thumbs-up), negative ("not creative," 30 trials; unlit bulb with thumbs-down), and neutral ("unevaluated," 15 trials; circle with question mark).

Each trial comprised two phases (Fig. 1A). During the feedback acquisition phase, a fixation screen (500 ms) was followed by the presentation of the participant's artwork and title (500 ms), the partner's name (1000 ms), and the partner's evaluation (3000 ms). The interstimulus interval was jittered around 2000 ms. In the evaluation phase, the partner's name and artwork were presented for 500 ms, after which two response options appeared. Participants judged the partner's artwork as either "creative" or "not creative" via a touchscreen response on the mobile device. The selected option was immediately highlighted. The intertrial interval lasted, on average, 3000 ms.

The objective creativity (OC) of the 75 artwork images was independently assessed by an additional sample (n = 33; 25 females; mean age = 22.64 ± 2.42 years). Each artwork was rated on a 5-point Likert scale (1 = "not creative at all," 5 = "very creative"). Based on mean ratings, artworks were classified into five OC levels (15 images per level). These OC levels were included as a within-subject factor in subsequent behavioral analyses (see Behavioral Data Analysis). To examine whether the gender imbalance introduced bias, independent-samples *t*-tests were conducted comparing male and female raters' scoring decisions. Although significant differences were initially found for two images, a gender-weighted reanalysis yielded identical OC category assignments, suggesting that no meaningful bias existed in the OC scores.

2.4. Neuropsychological assessments

Participants completed the following self-report questionnaires: the Brief Fear of Negative Evaluation Scale-II (BFNE-II), assessing apprehension and distress related to negative social judgment; the Rosenberg Self-Esteem Scale (RSES), measuring global self-esteem; the State Self-Esteem Scale (SSES), assessing situational fluctuations in self-esteem across performance, social, and appearance domains; and the Patient Health Questionnaire-9 (PHQ-9), a validated measure of depressive symptom severity. Internal consistency for each scale was assessed using Cronbach's alpha (α). Reliability coefficients were computed based on item-level responses within the present sample (n = 129). All analyses were conducted in R using the psych package. Missing values were handled using pairwise deletion. All scales demonstrated good-to-excellent internal consistency in the present sample (BFNE-II: α = .921; RSES: α = .872; SSES: α = .905; PHQ-9: α = .857).

Emotional valence and arousal responses to partner feedback were assessed using the Self-Assessment Manikin (SAM), presented on a visual analog scale ranging from 0 to 50. The valence scale depicted figures progressing from a sad, frowning face to a happy, smiling face, while the arousal scale illustrated figures ranging from a drowsy, relaxed state to an alert, highly excited state. These ratings were obtained retrospectively after the main task was completed, with each feedback image presented again for individual evaluation.

2.5. Behavioral data analysis

To examine how social feedback influenced participants' choices across levels of OC, we conducted a 3 × 5 repeated-measures analysis of variance (rmANOVA) on the percentage of "creative" choices, with feedback type (positive, negative, neutral) and OC (5 levels) as within-subject factors. Reaction times (RTs) were also analyzed to capture the dynamics of evaluative processing, beyond binary choice outcomes; specifically, the extent to which prior social feedback influenced the fluency of subsequent judgments. For RT analyses, trials with RTs exceeding ±2 SDs from each participant's mean were excluded to reduce the influence of outliers (Berger & Kiefer, 2021), as SD-based exclusion methods have been shown to introduce minimal bias while improving statistical sensitivity. This procedure excluded 4.5% of trials from both RT and choice analyses. Remaining RTs were standardized within participants across trials to account for individual differences in baseline response speed and variability, allowing for more accurate comparison of condition-specific effects. A 3 (feedback type) × 2 (decision type: "creative" vs. "not creative") rmANOVA was then conducted on RTs. Five participants who did not provide any "not creative" responses in the neutral feedback condition were excluded from the RT analysis owing to incomplete within-subject cell structure. Additionally, a 3 (feedback type) × 5 (OC) rmANOVA was performed on RTs, with results reported in Supplementary Text 1. A three-way rmANOVA including feedback type, OC, and decision type could not be performed due to insufficient trials per condition.

Valence and arousal ratings obtained from the SAM were analyzed

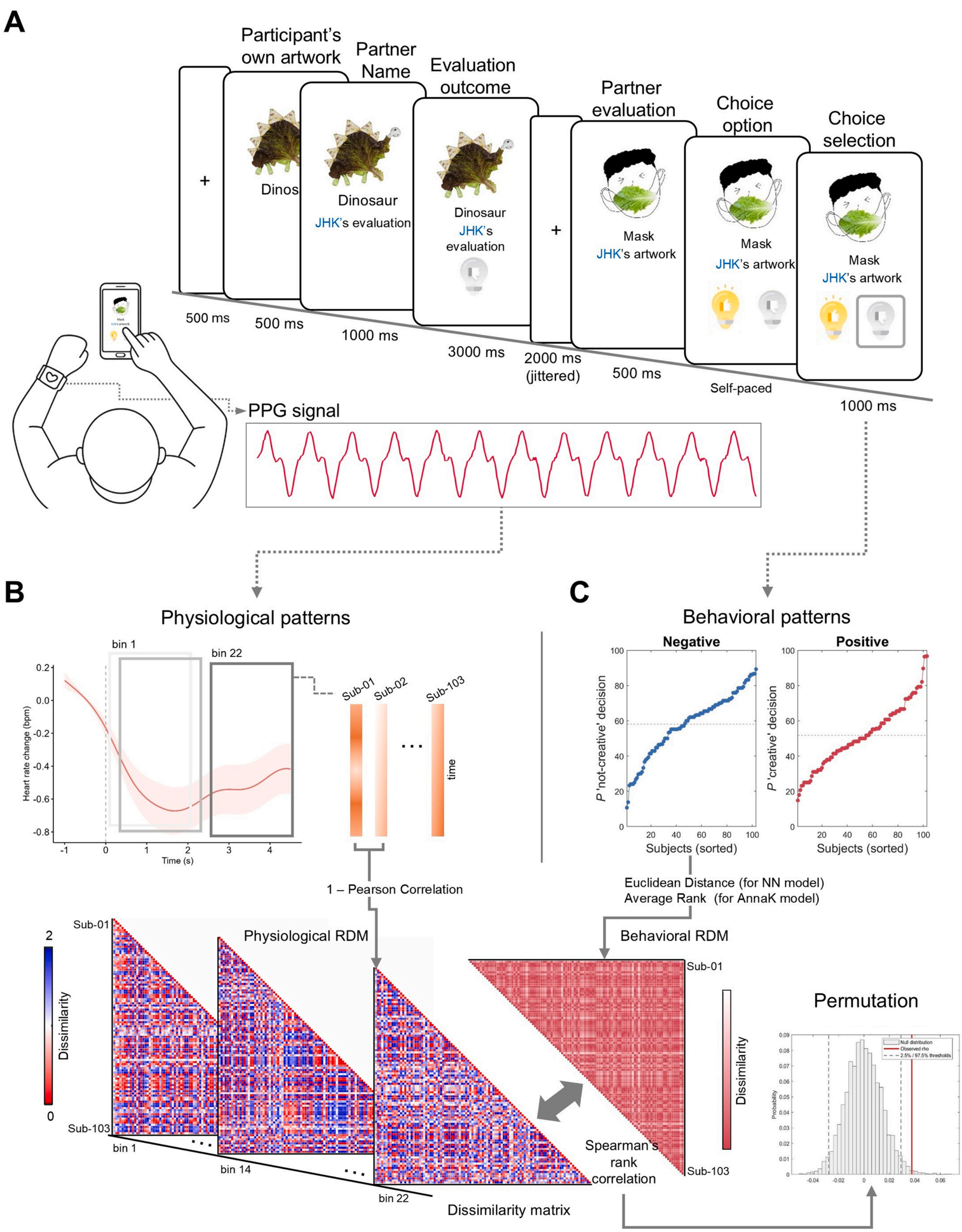

Fig. 1. Experimental overview and IS-RSA workflow. (A) Reciprocal artwork evaluation task. On each trial, participants received feedback on their artwork (positive, negative, or neutral) and subsequently evaluated the partner's artwork. Behavioral responses were collected on a mobile device, while raw photoplethysmography (PPG) signals were continuously recorded via a smartwatch. (B) Event-related cardiac time series were extracted from PPG signals and baseline-corrected to obtain heartbeat-evoked responses. (C) Behavioral indices of social evaluation were derived from participants' choices. (D) For each modality, condition-specific response patterns were converted into representational dissimilarity matrices. Physiological and behavioral RDMs were then compared using Spearman correlations, with intersubject similarity patterns further assessed through permutation testing and clustering analyses.

using one-way rmANOVAs with feedback type (positive, negative, neutral) as a within-subject factor to test whether perceived affective responses differed across conditions.

For all rmANOVAs, sphericity was assessed using Mauchly's test. When violated, Greenhouse–Geisser–corrected degrees of freedom and p-values were reported, along with the corresponding epsilon (ε). Significant main effects and interactions were followed by post hoc pairwise comparisons corrected for multiple testing. All analyses were conducted in R (version 4.2.3) using RStudio. Statistical significance was set at $P < .05$.

2.6. Physiological data analysis

2.6.1. Baseline heart rate variability analysis

Galaxy Watch cardiac data obtained during baseline HRV assessment were resampled to correct for irregular sampling rates using a custom Python function. The initial and final 30-s segments were discarded, yielding a 5-minute recording. Resampled ECG data were then preprocessed using the PhysioData Toolbox (version 0.6.3) (Sjak-Shie, 2022). Specifically, ECG signals were bandpass filtered between 1 and 50 Hz using a Butterworth filter. R-peaks were automatically detected, and missed or incorrectly identified peaks were manually corrected.

For HRV calculation, interbeat intervals (IBIs) were detrended using a smoothness-prior method (Tarvainen et al., 2002) with $\lambda = 500$. The root mean square of successive differences (RMSSD) was used as the primary time-domain index, as it is considered less susceptible to respiratory influences than frequency-domain HRV measures (Penttilä et al., 2001). However, recent methodological recommendations urge caution in attributing specific autonomic sources to HRV metrics and emphasize the importance of accounting for breathing when interpreting RMSSD as a parasympathetic index (Quigley et al., 2024; Ritz, 2024).

2.6.2. PPG-based evoked heart rate analysis

Preprocessing and evoked HR analyses of PPG data acquired during the artwork evaluation task were performed using the Systole package (Legrand & Allen, 2022). Raw signals were resampled at 1000 Hz and bandpass filtered using a Butterworth filter with cutoffs at 0.5 and 20 Hz. Systolic peaks were automatically detected using an improved Pan-Tompkins algorithm (Pan & Tompkins, 1985) and manually corrected for missed or misidentified peaks, a procedure well suited for time-locked analyses. IBIs were computed from corrected systolic peaks, and instantaneous HR time series (beats per minute; BPM) were estimated via interpolation.

Evoked HR was defined as time-locked fluctuations in instantaneous HR at feedback onset. To prevent potential physiological contamination from the following artwork presentation, four-and-a-half-second epochs were extracted for each trial, and HR changes were quantified relative to a 1-s prestimulus baseline. HR responses were analyzed using a one-way rmANOVA with feedback type as a within-subject factor. Post hoc multiple comparisons were corrected using the false discovery rate method. This window ensured that all analyzed cardiac responses occurred before the partner's artwork was presented. The full HR time course is provided in Supplementary Fig. S1. To further examine the temporal dynamics of feedback-related HR responses, an additional rmANOVA that included time as a within-subject factor was conducted using HR values averaged into 500-ms bins. Detailed results are reported in Supplementary Text 2.

Beyond examining the phasic cardiac responses to evaluative feedback, we exploratorily examined whether individual differences in resting HRV, indexed by RMSSD, were associated with the magnitude of feedback-evoked HR deceleration, given prior evidence that resting HRV reflects a baseline autonomic regulatory capacity associated with context-sensitive phasic cardiac reactivity (Lane et al., 2009; Park & Thayer, 2014)

2.7. Intersubject representational similarity analysis

IS-RSA was used to identify temporal cardiac patterns associated with individual differences in behavior under positive and negative feedback conditions. IS-RSA quantifies pairwise similarity in neural or physiological responses across individuals as a function of behavioral similarity (Chen et al., 2020; Finn et al., 2020). A schematic overview of the analysis is shown in Figs. 1B and 1C. All analyses were implemented in MATLAB R2020b (The MathWorks Inc., Natick, MA, USA) using custom scripts and the RSA toolbox (Nili et al., 2014).

2.7.1. Behavioral dissimilarity matrices

Behavioral dissimilarity matrices were constructed using two models: nearest neighbors (NN) and Anna Karenina (AnnaK). These models were selected because they are widely used, theoretically distinct approaches within IS-RSA research that capture complementary assumptions about how behavioral variation relates to similarity in cardiac response (Finn et al., 2020; Ilomäki et al., 2025; Kim & Kim, 2022; Yanagisawa et al., 2025; Zhang et al., 2025). The NN model assumes that participants with more similar behavioral scores are more alike, irrespective of their absolute position on the scale. Accordingly, pairwise Euclidean distances between participants were computed to generate the behavioral dissimilarity matrix (Fig. 1C and Fig. 4A).

In contrast, the AnnaK model, inspired by Tolstoy's dictum that "all happy families are alike; each unhappy family is unhappy in its own way," assumes asymmetry in similarity across the behavioral spectrum. Specifically, individuals at one end of the distribution (e.g., higher scores) may show greater similarity, whereas those at the opposite end exhibit greater idiosyncrasy (Finn et al., 2020). Unlike the NN model, which captures only relative distances, the AnnaK model incorporates absolute position on the behavioral dimension, thereby capturing the overall level of each dyad. The direction of this asymmetry can be specified based on the behavioral construct of interest. In the present study, we hypothesized that participants more strongly influenced by social feedback, those who judged partners' artwork more favorably following positive feedback or less favorably following negative feedback, would exhibit greater cardiac similarity (Fig. 4B). For the positive feedback condition, participants were ranked in descending order of their "creative" decision rates, with higher rates assigned lower rank values, and the behavioral matrix was defined as the mean rank for each participant pair. For the negative feedback condition, "not creative" decision rates were used, such that higher values reflected stronger unfavorable responding; participants were again ranked in descending order, and the behavioral matrix was defined as the mean rank of each dyad. In both conditions, positive correlations indicate that participants with stronger feedback-driven behavioral responses exhibited greater cardiac similarity, whereas negative correlations indicate the opposite pattern.

2.7.2. Physiological dissimilarity matrices

Physiological dissimilarity matrices were constructed using a 2200-ms sliding window (22 time points; 1-sample step size) starting from feedback onset and extending through the feedback presentation period (Zhang et al., 2025). This time-resolved approach was used to identify when cardiac responses were most strongly associated with behavioral indices. For each window, Pearson correlation coefficients were computed between pairs of event-evoked HR time series across participants and converted to dissimilarity matrices (1 – Pearson r), yielding 22 participant-by-participant physiological dissimilarity matrices per feedback valence (Fig. 1B). Robustness of these results to variations in sliding-window length was confirmed in Supplementary Text 3.

2.7.3. Model testing

At each time point, Spearman rank correlations were computed between the vectorized lower triangles of the physiological and behavioral dissimilarity matrices, separately for positive and negative feedback conditions. The neutral condition was excluded due to the limited number of trials.

Statistical significance was assessed using a Mantel permutation test (Mantel, 1967), implemented in MATLAB with the *bramila_mantel* functions (Glerean et al., 2016). At each iteration, subject labels were permuted by jointly shuffling rows and columns of one dissimilarity matrix, and the Spearman correlation was recalculated. This procedure was repeated 5000 times to generate a null distribution from which p-values were derived. Correlations exceeding the $P < .05$ threshold (one-tailed for NN; two-tailed for AnnaK) were corrected for multiple comparisons across sliding windows using the Benjamini–Hochberg false discovery rate procedure (Benjamini & Hochberg, 1995).

2.8. Exploratory computational modeling: value for self-protection

The same computational reinforcement learning model originally introduced in Yoon et al. (2018) was applied to estimate how the value of self-protective (VSP) evaluation was updated by integrating sequentially presented social feedback in moment-to-moment fashion. Building on the neural validity established in Yoon et al. (2018), we estimated trial-wise changes in self-defensive motivation and examined their correspondence with cardiac responses, extending the original findings from the neural to autonomic domains. In this computational model, VSP was updated on a trial-by-trial basis as a function of received feedback. On trial t, the updated value was defined as:

$$VSP(t) = VSP_t + \alpha \times [FB_t - VSP_{t-1}] \tag{1}$$

where α denotes an individual learning rate, treated as a free parameter estimated via optimization, and FB(t) represents the feedback received on trial t. The first trial was initialized with VSP(0) = 0. Updated VSP values were then passed through a softmax choice rule (Luce, 1959) to compute the probability of selecting a "creative" response.

Subject-specific VSP estimates were subsequently entered as predictors in a logistic regression model:

$$logit(P(y_i = \ 'creative')) = \beta_0 + \beta_{VSP} + \beta_{oc} \tag{2}$$

where D = 1 indicates that the participant evaluated the partner's artwork as creative and D = 0 otherwise. Unlike the maximum likelihood estimation approach used in Yoon et al. (2018), Bayesian estimation was employed in the present study as it provides full posterior distributions over parameters rather than point estimates. This enabled more principled uncertainty quantification and more stable parameter recovery (Kruschke, 2015). Logistic regression was implemented using Bayesian estimation in Stan package (version 2.32.6) via R software. The likelihood was specified as a Bernoulli distribution. A normal prior (mu = 0, σ = 1) was assigned to the intercept, and Student-t priors ($\nu = 3$, mu = 0, σ = 2.5) were specified for the VSP, OC, and subject-level learning rate parameters, with the learning rate constrained to the [0, 1] interval. These specifications followed the recommendations for logistic regression models (Gelman et al., 1995), as weakly informative prior specifications regularized parameter estimates without strongly constraining inference to prior expectations.

Model fitting was performed using Hamiltonian Markov chain Monte Carlo (MCMC) sampling implemented in Stan (version 2.9.0) to estimate the joint posterior distributions of model parameters for each participant. Each model was fit using four MCMC chains of 4000 iterations, including 1000 warm-up iterations, yielding 16,000 posterior samples per participant. Convergence was assessed using the Gelman-Rubin statistic, with all parameters meeting the criterion of being below 1.05.

To examine the effect of VSP on partner artwork evaluations, a paired t test was conducted comparing the percentage of "creative" decisions between high- and low-VSP trials. High and low-VSP levels were defined using ± 0.1 thresholds to reduce misclassification due to estimation variability around the neutral point, resulting in the exclusion of approximately 9.62% of trials. The distribution of feedback categories across VSP conditions showed marked asymmetry. In high-VSP trials, most trials followed negative feedback (95.71% ± 3.04%), with neutral and positive feedback accounting for 3.83% ± 1.34% and 0.46% ± 2.06% of trials, respectively. In contrast, low-VSP trials were primarily associated with positive feedback (70.83% ± 2.92%), with the remainder corresponding to neutral feedback (29.17% ± 2.94%). These results indicate that high-VSP states predominantly co-occurred with negative feedback, whereas low-VSP states were more evenly distributed across positive and neutral feedback.

Evoked HR analyses were also conducted to test whether cardiac responses differed as a function of VSP level, using paired t tests at each time bin of the heartbeat-evoked time series (FDR-corrected, $P < .05$). Finally, IS-RSA was applied to assess intersubject similarity between behavioral and cardiac response patterns. Results are reported in Supplementary Text 4.

2.9. Modality-based replication and cross-validation using research-grade electrocardiography

An independent cohort was recruited to validate PPG-derived cardiac findings against research-grade ECG recordings. Fifty-two participants (36 females; mean age = 23.17 ± 3.37 years; age range = 18–37 years) with no history of psychiatric or neurological disorders were enrolled. The study protocol was approved by the Institutional Review Board of Korea University, and written informed consent was obtained from all participants prior to participation. Participants received monetary compensation (KRW 20,000; approximately USD 16). Three participants were excluded from behavioral analyses: one due to E-prime data loss, and two were excluded due to cardiac irregularities characterized by repeated segments with missing R-peaks in the ECG signal. This resulted in a final sample of 49 participants.

Cardiac signals were recorded using a research-grade ECG system to enable modality-based replication of the main findings. ECG data were acquired with a BIOPAC Student Lab 4.1 system (BIOPAC Systems, Inc., Santa Barbara, CA, USA) at a sampling rate of 2000 Hz. Three-lead placements (LL, LA, RA), adapted from the Mason–Likar configuration, were used to minimize motion-related artifacts associated with task responses (Kligfield et al., 2007). Event triggers were transmitted to the BIOPAC system via the Chronos input device (Psychology Software Tools, USA) to ensure precise synchronization with task events.

ECG preprocessing, HRV computation, and event-evoked HR analyses followed the same procedures as those used in the main experiment with Galaxy Watch PPG data and are therefore not detailed here. The sole methodological addition in the ECG replication session was the concurrent acquisition of respiration signals, which were analyzed as described below.

Additionally, respiration was continuously monitored using a respiratory belt positioned around the upper chest. Thoracic expansion during breathing was transduced into a respiration signal. Respiration data from the HRV task were processed using the PhysioData Toolbox (Sjak-Shie, 2022) with standard belt-based settings, including low-pass filtering at 0.7 Hz and automated detection of inhalation and exhalation phases. Signals were visually inspected and manually corrected when necessary. For each predefined epoch aligned with ECG processing, the mean interpolated breath period was calculated and converted to respiration rate (breaths/minute) by dividing 60 by the breath period. Respiration rate was included to control for respiratory influences on ECG-derived HRV measures, given evidence that breathing patterns substantially affect the interpretation of time-domain HRV indices such as RMSSD (Quigley et al., 2024; Ritz, 2024).

Respiration signals acquired during the artwork evaluation task were processed using NeuroKit2's rsp_process function (Khodadad et al., 2018), which performs signal cleaning and automated detection of respiratory cycles. Preprocessed signals were segmented into event-related epochs time-locked to feedback onset (−1 to +6 s), and respiration rate changes were quantified relative to a one-second prestimulus baseline. Trial-wise mean respiration rate was used to assess feedback-related effects on respiration via one-way rmANOVA and to control for respiratory influences in correlation analyses between event-evoked HR deceleration and HRV indices.

To ensure procedural consistency across modalities, participants completed the same reciprocal artwork evaluation task as described above, with minor modifications. Specifically, the task comprised 100 trials, including 40 positive, 40 negative, and 20 neutral feedback trials. All other task parameters, including stimulus presentation, trial structure, and response requirements, were identical to those of the main experiment.

Behavioral data analysis and physiological preprocessing and analysis followed the same procedures as in the main experiment. The only exception concerned correlational analyses and IS-RSA, for which criteria were adjusted due to the smaller ECG replication sample. Given the limited statistical power for individual-level inference, uncorrected thresholds were primarily used to assess whether the main PPG findings were replicated, and these results were treated as exploratory evidence of consistency.

3. Results

3.1. Behavioral results

3.1.1. Effects of feedback and objective creativity on artwork evaluation

A 3 (feedback type: positive, negative, neutral) × 5 (OC levels: 1–5) rmANOVA on the percentage of “creative” choices revealed significant main effects of feedback type, $F(2, 256) = 51.27$, $p < .001$, $\eta^2_p = .286$, and OC level, $F(4, 512) = 486.46$, $p < .001$, $\varepsilon = 0.75$, $\eta^2_p = .792$. Participants were less likely to judge their partner’s artwork as creative after receiving negative feedback ($M_{NEG} = 42.61$, $SD_{NEG} = 18.22$) than after positive feedback ($M_{POS} = 52.86$, $SD_{POS} = 18.43$; $t(128) = 8.12$, $p < .001$) or neutral feedback ($M_{NEU} = 54.16$, $SD_{NEU} = 20.81$; $t(128) = 9.44$, $p < .001$). No significant difference was observed between positive and neutral feedback conditions, $t(128) = 1.03$, $p = .91$. Creative endorsements increased monotonically across OC levels, indicating that higher OC was associated with a greater likelihood of selecting the “creative” option. The feedback type × OC level interaction was also significant, $F(8, 1024) = 12.59$, $p = .001$, $\varepsilon = 0.89$, $\eta^2_p = 0.09$ (Fig. 2A). Follow-up simple main effects analyses showed that negative feedback consistently reduced “creative” responses relative to positive feedback across all OC levels (all $ps < .05$).

3.1.2. Effects of feedback and decision type on reaction time

A 3 (feedback type: positive, negative, neutral) × 2 (decision type: creative, not creative) rmANOVA on standardized RTs revealed significant main effects of feedback type, $F(2, 246) = 3.80$, $p = .027$, $\varepsilon = 0.92$, $\eta^2_p = .030$, and decision type, $F(1, 123) = 23.88$, $p < .001$, $\eta^2_p = .163$, as well as a significant interaction, $F(2, 246) = 13.13$, $p < .001$, $\eta^2_p = .096$ (Fig. 2B). Post hoc comparisons indicated that participants responded faster when making “not creative” judgments following negative feedback ($M_{NEG} = -0.134$, $SD_{NEG} = 0.363$) than following neutral ($M_{NEU} = 0.085$, $SD_{NEU} = 0.544$, $p < .001$) or positive feedback ($M_{POS} = 0.014$, $SD_{POS} = 0.425$, $p = .002$). No significant differences across feedback conditions were observed for “creative” judgments (all $ps > .09$).

3.1.3. Self-assessment Manikin ratings

SAM valence ratings confirmed successful affective manipulation. Participants reported more positive affect following positive feedback ($M_{POS} = 39.6$, $SD_{POS} = 6.49$) and more negative affect following negative feedback ($M_{NEG} = 16.3$, $SD_{NEG} = 6.00$), $t(129) = -23.70$, $p < .001$, $d = 3.71$, 95% CI [2.85, 4.58]. In contrast, arousal ratings did not differ across feedback conditions, $t(128) = -0.76$, $p = 0.45$, $d = 0.08$, 95% CI [−0.13, 0.29], indicating comparable arousal responses to positive ($M_{POS} = 23.7$, $SD_{POS} = 12.1$) and negative feedback ($M_{NEG} = 22.8$, $SD_{NEG} = 10.7$; Fig. 2C).

3.1.4. Relationship between behavioral indices and personality traits

Correlation analyses showed that the percentage of “creative” choices under negative feedback was negatively associated with depression scores (PHQ-9; $\rho(129) = -.217$, 95% CI [−.373, −.056], $p = .013$), positively associated with state self-esteem (SSES; $\rho(129) = .202$, 95% CI [.029,.355], $p = .021$) and trait self-esteem (RSES; $\rho(129) = .187$, 95% CI [.011,.348], $p = .034$). No significant associations were observed with the fear of negative evaluation (BFNE2; $\rho(129) = -.083$, 95% CI [−.259,.093], $p = .350$). Under positive and neutral feedback, behavioral responses showed no significant correlations with any of the

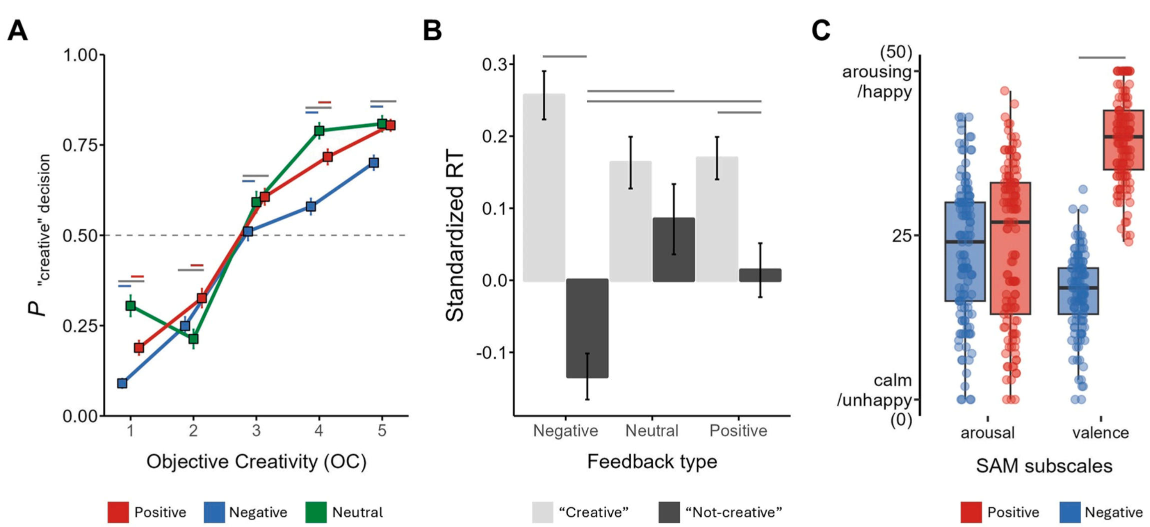

Fig. 2. Behavioral results. (A) Percentage of “creative” choices as a function of objective creativity (OC) level, plotted separately by feedback type. “Creative” choices increased monotonically with OC and were reduced following negative feedback relative to positive and neutral feedback. (B) Standardized reaction times (RTs) for “creative” and “not creative” decisions across feedback types. Participants were faster to reject partner artworks (“not creative” judgments) following negative feedback, whereas no feedback-related differences were observed for “creative” judgments. (C) Self-Assessment Manikin (SAM) ratings of arousal and valence as a function of feedback valence. Horizontal lines indicate significant post hoc pairwise comparisons (Tukey-corrected, $P < .05$).

examined personality measures (all $p > .20$). These findings indicate that individuals with higher depressive symptoms and lower self-esteem generally evaluated their partners' artworks more harshly following negative feedback.

3.2. Physiological results

3.2.1. Feedback-evoked heart rate responses

Fig. 3A illustrates instantaneous HR trajectories during the 4.5 seconds following feedback onset, shown in one-second increments. The waveforms depict changes in BPM over time for each feedback condition. A one-way rmANOVA revealed a significant effect of feedback valence on cardiac responses, with greater HR deceleration following negative feedback than following positive or neutral feedback.

Furthermore, the magnitude of HR deceleration in the negative feedback condition, averaged across the significant time window, was negatively correlated with RMSSD derived from ECG recordings ($r(103) = -.345$, 95% CI [−.505, −.162], $p < .001$; Fig. 3B). This association indicates that individuals with higher short-term HRV exhibited greater cardiac slowing in response to negative social feedback. To assess robustness to potential confounds, a multiple linear regression analysis was conducted including gender, age, BMI, sleep duration, alcohol consumption, and physical activity as covariates. RMSSD remained a significant predictor of HR deceleration ($\beta = -0.363$, $t(95) = -3.861$, $p < .001$), indicating that the observed relationship was not attributable to these demographic or lifestyle factors.

3.3. Intersubject representational similarity analysis using wearable PPG recording

To examine whether shared behavioral tendencies in response to social feedback were reflected in shared cardiac dynamics, IS-RSA was conducted between evoked HR time series and participants' proportions of decisions under positive and negative feedback, using both the NN and AnnaK models (Figs. 4C and 4D). The NN model did not reveal significant associations between behavioral and cardiac similarity in either feedback condition.

In contrast, the AnnaK model revealed a significant relationship in the positive feedback condition. Behavioral similarity, defined as similarity in "creative" decision rates, was positively correlated with similarity in evoked HR responses from 0.8 to 1.6 s following feedback onset. This finding indicates that individuals who were more strongly influenced by positive feedback exhibited more convergent cardiac responses during early feedback processing.

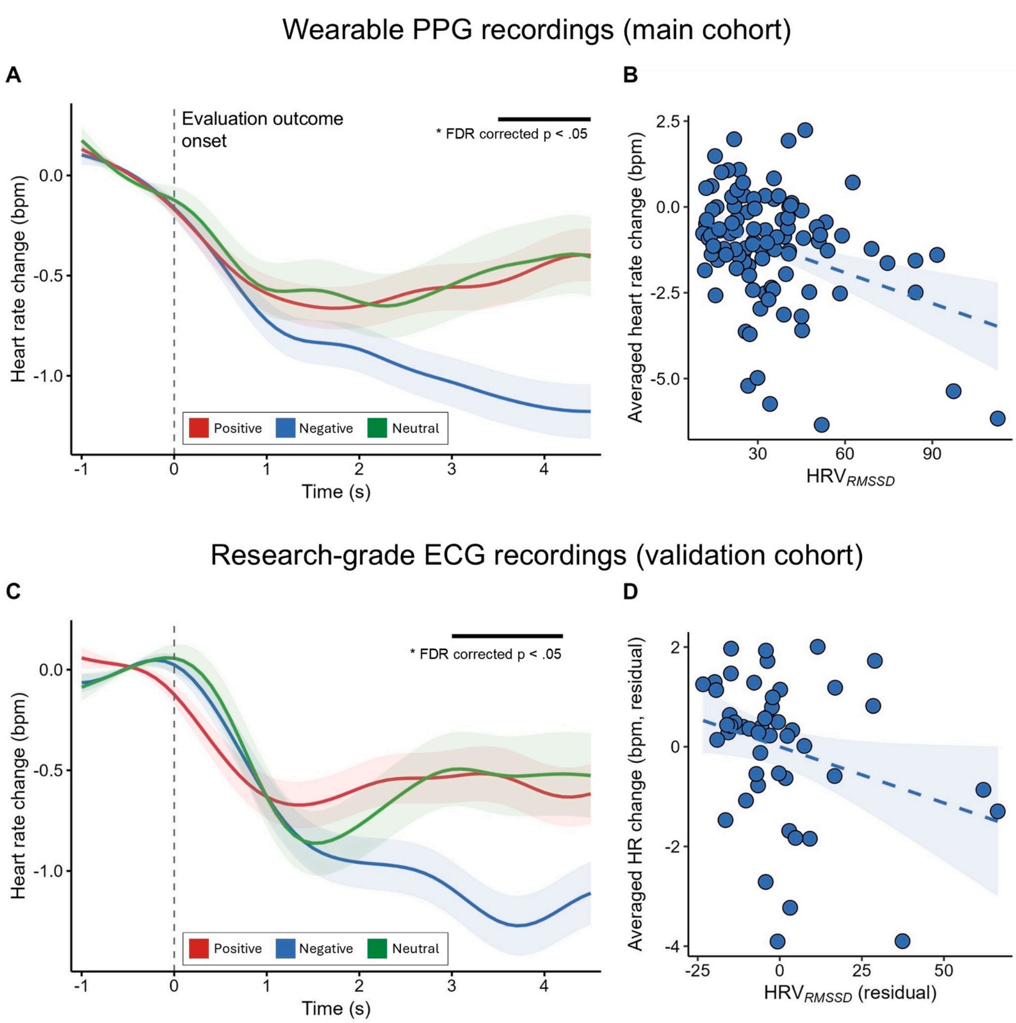

Fig. 3. Evoked heart rate analysis results using wearable PPG recordings (n = 103) and research-grade ECG recordings from a validation cohort (n = 49). (A, C) Heart rate responses as a function of feedback type derived from wearable PPG (A) and research-grade ECG (C) recordings. (B) Correlation between the HRV$_{RMSSD}$ index and mean heart rate change in the negative feedback condition. (D) Partial correlation between HRV$_{RMSSD}$ and mean heart rate change in the negative feedback condition, controlling for respiration rate. Shaded areas represent mean ± SEM across participants. Horizontal bars indicate time windows showing significant differences between conditions (FDR-corrected $p < .05$).

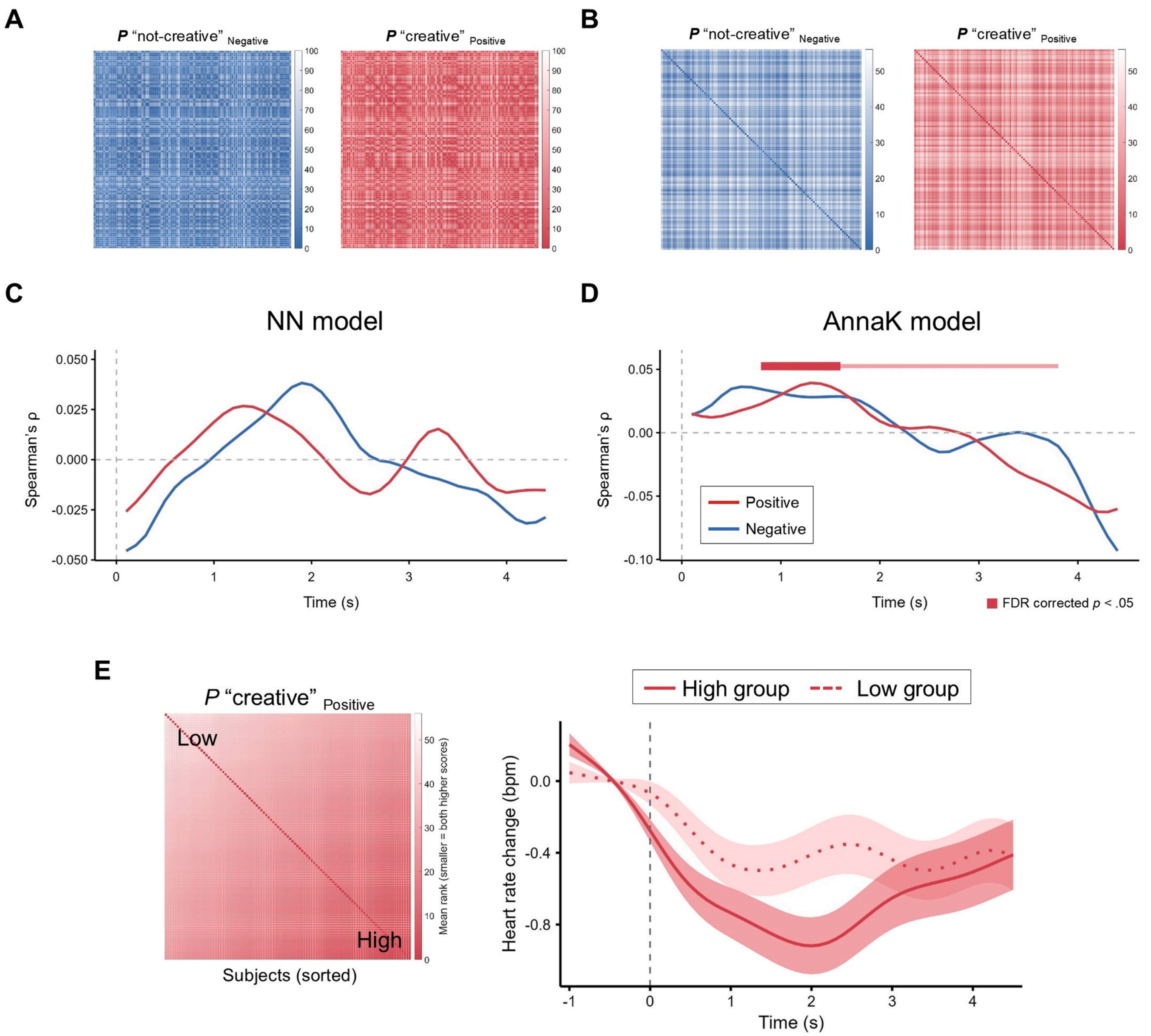

Fig. 4. Behavioral matrices and sliding-window IS-RSA results. (A) Behavioral dissimilarity matrices based on the nearest neighbors (NN) model (darker colors indicate greater similarity). (B) Behavioral dissimilarity matrices based on the Anna Karenina (AnnaK) model (darker colors indicate greater similarity at higher values). Time courses of similarity between heart rate responses and behavioral indices under the NN (C) and AnnaK (D) models. Horizontal bars denote significant IS-RSA windows (FDR-corrected $p < .05$). (E) The AnnaK behavioral similarity matrix, sorted by the percentage of "creative" decisions in the positive feedback condition (left), and the group-averaged HR time series for the high (n = 49) and low (n = 54) groups (right).

To further characterize this effect, participants were median-split into high- (n = 54) and low-sensitivity (n = 49) groups based on behavioral scores in the positive feedback condition. HR change trajectories (Fig. 4E) revealed that the high-sensitivity group tended to show greater HR deceleration, suggesting that heightened behavioral sensitivity to positive feedback is accompanied by a distinct physiological signature.

3.4. Cross-modal replication and validation using research-grade ECG recordings

Behavioral findings are reported in Supplementary Text 5 (Section 5.1). The behavioral tendency to devalue others' artwork following negative feedback was replicated.

3.4.1. Feedback-evoked heart rate responses and respiratory control

Consistent with the PPG findings, ECG-derived HR responses showed significantly greater deceleration following negative feedback compared to positive and neutral feedback (Fig. 3**C**). The temporal profile and relative magnitude of cardiac responses closely resembled those observed in the main physiological analyses. Peak deceleration occurred approximately one to two seconds after feedback onset, with condition differences persisting over several subsequent seconds. These results demonstrate strong convergence between ECG and PPG measurements, indicating that the observed cardiac modulation was not specific to wearable-based recordings.

To assess whether feedback-related cardiac deceleration was confounded by respiration, respiration rates were compared across feedback conditions. A one-way rmANOVA showed no significant differences in respiration rate ($F(2, 96) = 1.27$, $p = .284$, $\varepsilon = 0.97$, $\eta^2_p =$

.03), indicating that cardiac effects were not primarily driven by changes in breathing. Additionally, the negative association between RMSSD and HR deceleration in response to negative feedback was replicated ($\rho(49) = -.301$, 95% CI [−.566, −.001], $p = .036$; Fig. 3D) and remained significant after controlling for respiration rate, partial $\rho(49) = -.295$, $p = .042$.

3.4.2. Replication of IS-RSA patterns across modalities

Given the reduced sample size, IS-RSA results are reported at an uncorrected threshold in Supplementary Text 5 (Section 5.2) and should be interpreted as exploratory rather than confirmatory. Nevertheless, the observed pattern was qualitatively consistent with the AnnaK model identified in the PPG-based analyses.

4. Discussion

The present study investigated cardiac correlates of self-protective behavior in response to social evaluative feedback. Using wearable PPG and a sliding-window IS-RSA framework, we identified temporally specific cardiac signatures linking behavioral bias to interindividual similarity in HR dynamics during feedback processing. Behaviorally, participants evaluated their partners' artwork more harshly following negative feedback about their own work, and this self-protective bias was associated with higher depressive symptoms and lower self-esteem. Event-related analyses revealed stronger HR deceleration following negative feedback, with response magnitude further modulated by individual differences in an HRV index reflecting autonomic regulatory capacity. Finally, IS-RSA results were consistent with the AnnaK model: positive feedback elicited convergent cardiac response patterns characterized by HR deceleration among participants who showed stronger favorable evaluation bias. To our knowledge, this study is the first to apply a dynamic IS-RSA approach to wearable cardiac data, demonstrating that HR trajectories capture both shared and individual-specific autonomic signatures of motivational bias during social evaluation.

The behavioral results provide clear evidence of a self-protective bias, replicating the result of a previous neuroimaging study (Yoon et al., 2018) in which participants were more likely to derogate others' performance after receiving negative social feedback. This pattern was further supported by reinforcement learning modeling, which showed that trial-by-trial fluctuations in self-protective value (VSP) influenced partner evaluations, consistent with accounts proposing that social criticism engages defensive mechanisms aimed at restoring self-worth (Bourgeois & Leary, 2001; Coleman et al., 1987; Rodman et al., 2017). Notably, these VSPs have previously been shown to be tracked by the medial prefrontal cortex to guide adaptive behavioral responses under social-evaluative threat (Yoon et al., 2018). Moreover, individuals with lower self-esteem or higher depressive symptoms are known to exhibit heightened sensitivity to social rejection (Leary & Baumeister, 2000; Weightman et al., 2014), often engaging in other-derogation (e.g., devaluing others' performance or attributes) as a defensive strategy (Ford & Collins, 2010). Our exploratory finding that stronger self-protective bias toward unfavorable judgments under negative feedback was associated with higher depressive symptoms and lower self-esteem tentatively supports for this framework. In contrast, although it was closely related to depressive symptoms and poor self-esteem, the fear of negative evaluation was not associated with self-protective behavior, suggesting that this defensive response is more closely linked to internal affective vulnerability than concerns about others' judgments.

Phasic HR deceleration is widely interpreted as a parasympathetically mediated orienting response reflecting heightened vigilance and attentional engagement toward socially salient or threatening cues (Bradley et al., 2001; Ilves & Surakka, 2012; Patron et al., 2019). This transient deceleration is thought to facilitate information sampling under evaluative threat, enabling more effective monitoring of environmental cues (Lacey, 1967; Porges & Raskin, 1969). In the present study, stronger and more sustained HR deceleration was observed following negative feedback than following neutral or positive feedback. Whereas HR deceleration after positive or neutral feedback began to recover approximately two seconds after feedback onset, HR deceleration following negative feedback persisted throughout the five-second feedback window. A comparable pattern emerged when trials were categorized by self-protective value, with high-VSP trials showing greater HR deceleration than low-VSP trials (see Supplementary Fig. S3), further reinforcing the link between self-protective motivation and autonomic regulation. These findings are consistent with those of studies demonstrating cardiac slowing following social rejection or feedback indicating others' dislike (Dekkers et al., 2015; Gunther Moor et al., 2010; Van der Veen et al., 2014; van der Veen et al., 2016). Given that feedback regarding one's creative competence represents a distinct dimension of social evaluation that can independently affect self-esteem (Leary et al., 2001), these findings provide novel evidence that cardiac slowing to social-evaluative threat is not confined to social rejection but extends to ability-based evaluative feedback regarding one's creative competence.

Importantly, the magnitude of HR deceleration was associated with individual differences in resting HRV RMSSD, with higher HRV predicting stronger cardiac slowing in response to negative social feedback. This association was replicated in an independent dataset with concurrent ECG and respiratory recordings and remained significant after controlling for respiration rate. Considering that RMSSD is commonly interpreted as partially reflecting parasympathetic (vagal) activity, these findings align with theoretical accounts suggesting that parasympathetic flexibility supports adaptive coping under stress (Park & Thayer, 2014; Villringer et al., 2025). Those with a greater baseline autonomic regulatory capacity may possess greater vagal resources, enabling a more pronounced parasympathetic response when confronted with socially threatening stimuli. Notably, these observed HR deceleration effects were captured using PPG-derived HR data from commercially available wearable devices used in conjunction with a smartphone-based behavioral paradigm, underscoring the feasibility of high-resolution autonomic measurement in ecologically valid contexts.

A key methodological contribution of this study is the application of multivariate IS-RSA to wearable-derived HR data, allowing identification of shared temporal cardiac patterns linking behavioral tendencies to feedback-evoked dynamics. Notably, the association between behavioral bias and HR responses did not reflect the symmetric correspondence predicted by the NN model. Instead, the significant relationship observed under the AnnaK model revealed an asymmetric convergence pattern: participants exhibiting stronger behavioral bias toward favorable evaluations showed more convergent HR responses characterized by sustained deceleration, whereas those with weaker biases displayed more idiosyncratic cardiac patterns. This asymmetric convergence emerged during positive feedback and in trials marked by lower self-protective motivation. Importantly, these effects were observed within early post-feedback intervals identified by the IS-RSA analysis. It is worth noting that although the earliest significant IS-RSA window began at 0.8 s post-feedback onset, each window spanned 2200 ms with the HR intervals contributing to these effects extending from 0.8 to 3.0 s to 1.6–3.8 s post-feedback. Given that research has consistently reported HR deceleration within the first 1–2 s following the onset of evaluative feedback (Crone et al., 2003; Osumi & Ohira, 2009; Van der Veen et al., 2014), these windows substantially overlapped with the established time course of cardiac responses, supporting the temporal plausibility of the observed effects. While condition-level HR differences emerged around 3.5 s post-feedback onset, the IS-RSA revealed notable behavioral-cardiac correspondence at earlier time points. This suggests that cardiac responses associated with individual differences in behavioral bias may emerge earlier than those reflected in group-level condition effects.

Although HR deceleration is often interpreted as a defensive response to aversive stimuli, prior research shows that comparable deceleration can also occur in response to pleasant or rewarding stimuli (Bradley et al., 2001; Sánchez-Navarro et al., 2006). For example, Bradley et al. (2001) demonstrated stronger HR deceleration for highly arousing pleasant images, suggesting that cardiac slowing reflects heightened attentional or motivational engagement. In the present study, positive and negative feedback were rated as equally arousing on the SAM scale, indicating comparable physiological activation across valence. Within this context, HR deceleration during positive feedback may reflect affiliative or approach-related motivation. Overall, the IS-RSA findings delineate autonomic mechanisms associated with self-protective motivation and clarify how behavioral bias is organized at the interindividual physiological processes.

In contrast, no significant correspondence between behavioral bias and HR dynamics was observed under negative feedback or high self-protection motivation. This null effect may reflect a relatively uniform defensive physiological response to negative stimuli, as HR deceleration has been consistently reported in aversive and evaluative contexts (Battaglia et al., 2024; Boukarras et al., 2022; Gunther Moor et al., 2010). In the present data, negative feedback elicited robust HR deceleration at the group level, indicating broadly shared parasympathetic engagement. Because this response was highly synchronized across participants, interindividual variability in HR dynamics was reduced, limiting the sensitivity of IS-RSA to detect structured associations with behavioral tendencies. Thus, when physiological responses to social threat are already uniform, behavioral differences are less likely to be reflected in cardiac similarity patterns.

In contrast, positive feedback elicited more heterogeneous autonomic responses, with convergent HR patterns emerging only among individuals showing stronger favorable evaluation bias. This pattern suggests that physiological similarity arises selectively among individuals sharing approach-oriented motivational states. Consistent with the broaden-and-build theory of positive emotion (Fredrickson, 1998), positive affect may promote flexible and socially engaged responding, manifesting as greater overall autonomic variability but convergence among individuals with heightened approach motivation. Supporting this view, Iyer et al. (2024) showed using IS-RSA that negative social experiences produced homogeneous neural representations, whereas positive experiences yielded more idiosyncratic patterns, particularly in the ventromedial prefrontal cortex (vmPFC). Given evidence that the vmPFC integrates emotional valuation with autonomic regulation (Dundon et al., 2021; Hänsel & von Känel, 2008), together with our prior fMRI findings using the same paradigm (Yoon et al., 2018), these results suggest that vmPFC-mediated integration may underlie the observed valence-dependent asymmetry: negative feedback-evoked uniform defensive responses, whereas positive feedback permitted differentiated engagement shaped by individual motivational differences.

Several limitations should be noted. First, although the wearable-based implementation enhanced ecological validity, the experimental setting remained structured and may not fully capture the complexity of real-world social interactions. Future studies should extend this approach to more naturalistic contexts to examine how feedback-related HR responses unfold in everyday social settings. Second, although findings were replicated using research-grade ECG and respiratory rate was controlled, HR dynamics reflect the combined influence of sympathetic and parasympathetic activity. While this reduces the likelihood of respiratory confounds, future studies should incorporate multimodal autonomic measures (e.g., electrodermal activity or blood pressure variability) to better dissociate underlying mechanisms. Finally, although IS-RSA revealed systematic convergence between behavioral and physiological patterns, causal inference remains limited. Intervention-based designs (e.g., biofeedback or vagal stimulation) may help clarify how behavioral-autonomic alignment evolves over time.

5. Conclusions

This study provides novel evidence that HR dynamics reflect variations in self-protective motivation during social evaluative feedback. Negative feedback elicited uniform HR deceleration, consistent with parasympathetic engagement, whereas positive feedback produced differentiated yet convergent cardiac patterns among individuals with stronger affiliative behavioral bias. These findings suggest that cardiac dynamics capture both shared and individual-specific signatures of social evaluative processing. Methodologically, applying IS-RSA to wearable-derived HR data offers a promising framework for identifying temporally organized behavioral–physiological correspondences beyond traditional univariate approaches. Collectively, these results advance understanding of autonomic mechanisms underlying self-protective behavior in social contexts and highlight a pathway for integrating laboratory-based psychophysiological approaches with mobile assessments of emotion regulation in daily life.

CRediT authorship contribution statement

Jinhee Kim: Writing – review & editing, Writing – original draft, Visualization, Validation, Project administration, Methodology, Investigation, Funding acquisition, Formal analysis, Data curation, Conceptualization. **Meeseung Lee:** Writing – review & editing, Project administration, Data curation, Conceptualization. **Daon Lee:** Writing – review & editing, Project administration, Investigation, Data curation. **Minyoung Kim:** Writing – review & editing, Project administration, Investigation, Data curation. **Hackjin Kim:** Writing – review & editing, Supervision, Project administration, Funding acquisition, Conceptualization.

Funding

This research was supported by the National Research Foundation (NRF) funded by the Korean government (MSIT) (NRF-2021M3A9E4080780; RS-2025-16072267), and by the Basic Science Research Program through the NRF funded by the Ministry of Education (2020R1I1A1A01070413; RS-2023-00241694).

Declaration of Generative AI and AI-assisted technologies in the writing process

During preparation of this work, the author(s) used ChatGPT to correct grammatical and spelling errors and improve readability of the manuscript. The author(s) subsequently reviewed and edited the content and take full responsibility for the publication.

Declaration of Competing Interest

H.K., J.K., and M.L. have a pending Korean patent application (No. 10-2024-0133081, filed September 30, 2024) related to the mobile application used for data collection in this study.

Appendix A. Supporting information

Supplementary data associated with this article can be found in the online version at doi:10.1016/j.biopsycho.2026.109278.

Data availability

Data will be made available on request.

References

Battaglia, S., Nazzi, C., Lonsdorf, T. B., & Thayer, J. F. (2024). Neuropsychobiology of fear-induced bradycardia in humans: Progress and pitfalls. *Molecular Psychiatry, 29*(12), 3826–3840. https://doi.org/10.1038/s41380-024-02600-x

Benjamini, Y., & Hochberg, Y. (1995). Controlling the false discovery rate: A practical and powerful approach to multiple testing. *Journal of the Royal Statistical society: Series B (Methodological), 57*(1), 289–300. https://doi.org/10.1111/j.2517-6161.1995.tb02031.x

Berger, A., & Kiefer, M. (2021). Comparison of different response time outlier exclusion methods: A simulation study. *Frontiers in Psychology, 12*, Article 675558. https://doi.org/10.3389/fpsyg.2021.675558

Boukarras, S., Garfinkel, S. N., & Critchley, H. D. (2022). Cardiac deceleration following positive and negative feedback is influenced by competence-based social status. *Social Neuroscience, 17*(2), 170–180. https://doi.org/10.1080/17470919.2022.2050295

Bourgeois, K. S., & Leary, M. R. (2001). Coping with rejection: Derogating those who choose us last [article]. *Motivation and Emotion, 25*(2), 101–111. https://doi.org/10.1023/A:1010661825137

Bradley, M. M., Codispoti, M., Cuthbert, B. N., & Lang, P. J. (2001). Emotion and motivation I: Defensive and appetitive reactions in picture processing. *Emotion, 1*(3), 276–298. https://doi.org/10.1037/1528-3542.1.3.276

Campbell, B. A., Wood, G., & McBride, T. (2013). Origins of orienting and defensive responses: An evolutionary perspective. In *Attention and orienting* (pp. 42–67). Psychology Press.

Candia-Rivera, D., Catrambone, V., Thayer, J. F., Gentili, C., & Valenza, G. (2022). Cardiac sympathetic-vagal activity initiates a functional brain–body response to emotional arousal. *Proceedings of the National Academy of Sciences, 119*(21), Article e2119599119. https://doi.org/10.1073/pnas.2119599119

Chen, P.-H. A., Jolly, E., Cheong, J. H., & Chang, L. J. (2020). Intersubject representational similarity analysis reveals individual variations in affective experience when watching erotic movies. *Neuroimage, 216*, 116851. https://doi.org/10.1016/j.neuroimage.2020.116851

Chen, J., Leong, Y. C., Honey, C. J., Yong, C. H., Norman, K. A., & Hasson, U. (2017). Shared memories reveal shared structure in neural activity across individuals. *Nature Neuroscience, 20*(1), 115–125. https://doi.org/10.1038/nn.4450

Coleman, L. M., Jussim, L., & Abraham, J. (1987). Students' reactions to teachers' evaluations: The unique impact of negative feedback. *Journal of Applied Social Psychology, 17*(12), 1051–1070. https://doi.org/10.1111/j.1559-1816.1987.tb02347.x

Crone, E. A., van der Veen, F. M., van der Molen, M. W., Somsen, R. J., van Beek, B., & Jennings, J. R. (2003). Cardiac concomitants of feedback processing. *Biological Psychology, 64*(1-2), 143–156. https://doi.org/10.1016/s0301-0511(03)00106-6

Dekkers, L. M., van der Molen, M. J., Gunther Moor, B., van der Veen, F. M., & van der Molen, M. W. (2015). Cardiac and electro-cortical concomitants of social feedback processing in women. *Social Cognitive and Affective Neuroscience, 10*(11), 1506–1514. https://doi.org/10.1093/scan/nsv039

Dundon, N. M., Shapiro, A. D., Babenko, V., Okafor, G. N., & Grafton, S. T. (2021). Ventromedial prefrontal cortex activity and sympathetic allostasis during value-based ambivalence. *Frontiers in Behavioral Neuroscience, 15*, Article 615796. https://doi.org/10.3389/fnbeh.2021.615796

Finn, E. S., Glerean, E., Khojandi, A. Y., Nielson, D., Molfese, P. J., Handwerker, D. A., & Bandettini, P. A. (2020). Idiosynchrony: From shared responses to individual differences during naturalistic neuroimaging. *Neuroimage, 215*, Article 116828. https://doi.org/10.1016/j.neuroimage.2020.116828

Ford, M. B., & Collins, N. L. (2010). Self-esteem moderates neuroendocrine and psychological responses to interpersonal rejection. *Journal of Personality and Social Psychology, 98*(3), 405. https://doi.org/10.1037/a0017345

Fredrickson, B. L. (1998). What good are positive emotions? *Review of General Psychology, 2*(3), 300–319. https://doi.org/10.1037/1089-2680.2.3.300

Gelman, A., Carlin, J. B., Stern, H. S., & Rubin, D. B. (1995). *Bayesian data analysis*. Chapman and Hall/CRC.

Glerean, E., Pan, R. K., Salmi, J., Kujala, R., Lahnakoski, J. M., Roine, U., Nummenmaa, L., Leppämäki, S., Nieminen-von Wendt, T., & Tani, P. (2016). Reorganization of functionally connected brain subnetworks in high-functioning autism. *Human Brain Mapping, 37*(3), 1066–1079. https://doi.org/10.1002/hbm.23084

Gunther Moor, B., Crone, E. A., & van der Molen, M. W. (2010). The heartbrake of social rejection: Heart rate deceleration in response to unexpected peer rejection. *Psychological Science, 21*(9), 1326–1333. https://doi.org/10.1177/0956797610379236

Hänsel, A., & von Känel, R. (2008). The ventro-medial prefrontal cortex: A major link between the autonomic nervous system, regulation of emotion, and stress reactivity? *Biopsychosocial Medicine, 2*(1), 1–5. https://doi.org/10.1186/1751-0759-2-21

Ilomäki, M., Lindblom, J., Flykt, M., Vänskä, M., Punamäki, R. L., & Wikman, P. (2025). Similarity in early life stress exposure is associated with similarity in neural representations in early adulthood. *Human Brain Mapping, 46*(14), Article e70373. https://doi.org/10.1002/hbm.70373

Ilves, M., & Surakka, V. (2012). Heart rate responses to synthesized affective spoken words. *Advances in Human-Computer Interaction, 2012*(1), Article 158487. https://doi.org/10.1155/2012/158487

Iyer, S., Collier, E., Broom, T. W., Finn, E. S., & Meyer, M. L. (2024). Individuals who see the good in the bad engage distinctive default network coordination during post-encoding rest. *Proceedings of the National Academy of Sciences, 121*(1), Article e2306295121. https://doi.org/10.1073/pnas.2306295121

Khodadad, D., Nordebo, S., Müller, B., Waldmann, A., Yerworth, R., Becher, T., … Miedema, M. (2018). Optimized breath detection algorithm in electrical impedance tomography. *Physiological Measurement, 39*(9), Article 094001. https://doi.org/10.1088/1361-6579/aad7e6

Kim, W., & Kim, M. J. (2022). Morphological similarity of amygdala-ventral prefrontal pathways represents trait anxiety in younger and older adults. *Proceedings of the National Academy of Sciences, 119*(42), Article e2205162119. https://doi.org/10.1073/pnas.2205162119

Kligfield, P., Gettes, L. S., Bailey, J. J., Childers, R., Deal, B. J., Hancock, E. W., … Mirvis, D. M. (2007). Recommendations for the standardization and interpretation of the electrocardiogram: Part I: The electrocardiogram and its technology: A scientific statement from the American Heart Association Electrocardiography and Arrhythmias Committee, Council on Clinical Cardiology; the American College of Cardiology Foundation; and the Heart Rhythm Society endorsed by the International Society for Computerized Electrocardiology. *Circulation, 115*(10), 1306–1324. https://doi.org/10.1161/CIRCULATIONAHA.106.180200

Klorman, R., Weissberg, R. P., & Wiesenfeld, A. R. (1977). Individual differences in fear and autonomic reactions to affective stimulation. *Psychophysiology, 14*(1), 45–51. https://doi.org/10.1111/j.1469-8986.1977.tb01154.x

Kruschke, J. (2015). *Doing Bayesian data analysis: A tutorial with R, JAGS, and Stan* (2nd ed.). Waltham, MA: Academic Press.

Lacey, J. (1967). *Somatic response patterning and stress: Some revisions of activation theory.* In M. H. Appley, & R. Trumbell (Eds.) (pp. 14–37). New York: Psychological Stress, Appleton-Century-Crofts.

Lane, R. D., McRae, K., Reiman, E. M., Chen, K., Ahern, G. L., & Thayer, J. F. (2009). Neural correlates of heart rate variability during emotion. *Neuroimage, 44*(1), 213–222. https://doi.org/10.1016/j.neuroimage.2008.07.056

Leary, M. R., & Baumeister, R. F. (2000). The nature and function of self-esteem: Sociometer theory [article]. *Advances in Experimental Social Psychology, 32*, 1–62. https://doi.org/10.1016/s0065-2601(00)80003-9

Leary, M. R., Cottrell, C. A., & Phillips, M. (2001). Deconfounding the effects of dominance and social acceptance on self-esteem. *Journal of Personality and Social Psychology, 81*(5), 898. https://doi.org/10.1037/0022-3514.81.5.898

Legrand, N., & Allen, M. (2022). Systole: A python package for cardiac signal synchrony and analysis. *Journal of Open Source Software, 7*(69), 3832. https://doi.org/10.21105/joss.03832

Luce, R. D. (1959). *Individual choice behavior, 4*. New York: Wiley.

Mantel, N. (1967). The detection of disease clustering and a generalized regression approach. *Cancer Research, 27*(2), 209–220.

Moore, R. C., Swendsen, J., & Depp, C. A. (2017). Applications for self-administered mobile cognitive assessments in clinical research: A systematic review. *International Journal of Methods in Psychiatric Research, 26*(4), Article e1562. https://doi.org/10.1002/mpr.1562

Nguyen, M., Vanderwal, T., & Hasson, U. (2019). Shared understanding of narratives is correlated with shared neural responses. *Neuroimage, 184*, 161–170. https://doi.org/10.1016/j.neuroimage.2018.09.010

Nili, H., Wingfield, C., Walther, A., Su, L., Marslen-Wilson, W., & Kriegeskorte, N. (2014). A toolbox for representational similarity analysis. *PLoS Computational Biology, 10*(4), Article e1003553. https://doi.org/10.1371/journal.pcbi.1003553

Noordewier, M. K., Scheepers, D. T., & Hilbert, L. P. (2020). Freezing in response to social threat: A replication. *Psychological Research, 84*(7), 1890–1896. https://doi.org/10.1007/s00426-019-01203-4

Osumi, T., & Ohira, H. (2009). Cardiac responses predict decisions: An investigation of the relation between orienting response and decisions in the ultimatum game. *International Journal of Psychophysiology, 74*(1), 74–79. https://doi.org/10.1016/j.ijpsycho.2016.09.017

Osumi, T., & Ohira, H. (2016). Heart-rate deceleration predicting the determination of costly punishment: Implications for its involvement in cognitive effort expended in overriding self-interest. *International Journal of Psychophysiology, 109*, 29–36. https://doi.org/10.1016/j.ijpsycho.2016.09.017

Pan, J., & Tompkins, W. J. (1985). A real-time QRS detection algorithm. *IEEE Transactions on Biomedical Engineering, 32*(3), 230–236. https://doi.org/10.1109/TBME.1985.325532

Park, G., & Thayer, J. F. (2014). From the heart to the mind: Cardiac vagal tone modulates top-down and bottom-up visual perception and attention to emotional stimuli. *Frontiers in Psychology, 5*, 278. https://doi.org/10.3389/fpsyg.2014.00278

Patron, E., Mennella, R., Benvenuti, S. M., & Thayer, J. F. (2019). The frontal cortex is a heart-brake: Reduction in delta oscillations is associated with heart rate deceleration. *Neuroimage, 188*, 403–410. https://doi.org/10.1016/j.neuroimage.2018.12.035

Penttilä, J., Helminen, A., Jartti, T., Kuusela, T., Huikuri, H. V., Tulppo, M. P., Coffeng, R., & Scheinin, H. (2001). Time domain, geometrical and frequency domain analysis of cardiac vagal outflow: Effects of various respiratory patterns. *Clinical Physiology, 21*(3), 365–376. https://doi.org/10.1046/j.1365-2281.2001.00337.x

Porges, S. W., & Raskin, D. C. (1969). Respiratory and heart rate components of attention. *Journal of Experimental Psychology, 81*(3), 497. https://doi.org/10.1037/h0027921

Quigley, K. S., Gianaros, P. J., Norman, G. J., Jennings, J. R., Berntson, G. G., & de Geus, E. J. C. (2024). Publication guidelines for human heart rate and heart rate variability studies in psychophysiology-Part 1: Physiological underpinnings and foundations of measurement. *Psychophysiology, 61*(9), Article e14604. https://doi.org/10.1111/psyp.14604

Ritz, T. (2024). How to account for respiration in respiratory sinus arrhythmia: Publication standards for heart rate variability studies in Biological Psychology. *Biological Psychology, 190*, Article 108806. https://doi.org/10.1016/j.biopsycho.2024.108806

Rodman, A. M., Powers, K. E., & Somerville, L. H. (2017). Development of self-protective biases in response to social evaluative feedback. *Proceedings of the National Academy of Sciences, 114*(50), 13158–13163. https://doi.org/10.1073/pnas.1712398114

Roelofs, K., Hagenaars, M. A., & Stins, J. (2010). Facing freeze: Social threat induces bodily freeze in humans. *Psychological Science, 21*(11), 1575–1581. https://doi.org/10.1177/0956797610384746

Sánchez-Navarro, J. P., Martinez-Selva, J. M., & Román, F. (2006). Uncovering the relationship between defence and orienting in emotion: Cardiac reactivity to unpleasant pictures. *International Journal of Psychophysiology, 61*(1), 34–46. https://doi.org/10.1016/j.ijpsycho.2005.10.023

Sjak-Shie, E.E. (2022). *PhysioData toolbox (version 0.6.3)*. In Retrieved from ⟨https://PhysioDataToolbox.leidenuniv.nl⟩.

Stieger, S., Lewetz, D., & Reips, U.-D. (2018). Can smartphones be used to bring computer-based tasks from the lab to the field? A mobile experience-sampling method study about the pace of life. *Behavior Research Methods, 50*(6), 2267–2275. https://doi.org/10.3758/s13428-017-0991-6

Tarvainen, M. P., Ranta-Aho, P. O., & Karjalainen, P. A. (2002). An advanced detrending method with application to HRV analysis. *IEEE Transactions on Biomedical Engineering, 49*(2), 172–175. https://doi.org/10.1109/10.979357

Triana, A. M., Salmi, J., Hayward, N. M. E. A., Saramäki, J., & Glerean, E. (2024). Longitudinal single-subject neuroimaging study reveals effects of daily environmental, physiological, and lifestyle factors on functional brain connectivity. *PLoS Biology, 22*(10), Article e3002797. https://doi.org/10.1371/journal.pbio.3002797

Tutunji, R., Kogias, N., Kapteijns, B., Krentz, M., Krause, F., Vassena, E., & Hermans, E. J. (2023). Detecting prolonged stress in real life using wearable biosensors and ecological momentary assessments: Naturalistic experimental study. *Journal of Medical Internet Research, 25*, Article e39995. https://doi.org/10.2196/39995

van der Veen, F. M., van der Molen, M. J. W., van der Molen, M. W., & Franken, I. H. A. (2016). Thumbs up or thumbs down? Effects of neuroticism and depressive symptoms on psychophysiological responses to social evaluation in healthy students. *Cognitive, Affective, & Behavioral Neuroscience, 16*(5), 836–847. https://doi.org/10.3758/s13415-016-0435-2

Van der Veen, F. M., van der Molen, M. W., Sahibdin, P. P., & Franken, I. H. (2014). The heart-break of social rejection versus the brain wave of social acceptance. *Social Cognitive and Affective Neuroscience, 9*(9), 1346–1351. https://doi.org/10.1093/scan/nst120

Villringer, A., Nikulin, V. V., & Gaebler, M. (2025). Brain–body states as a link between cardiovascular and mental health. *Trends in Neurosciences, 48*(10), 766–779. https://doi.org/10.1016/j.tins.2025.08.004

Wang, R., Yu, R., Tian, Y., & Wu, H. (2022). Individual variation in the neurophysiological representation of negative emotions in virtual reality is shaped by sociability. *Neuroimage, 263*, Article 119596. https://doi.org/10.1016/j.neuroimage.2022.119596

Weightman, M. J., Air, T. M., & Baune, B. T. (2014). A review of the role of social cognition in major depressive disorder. *Frontiers in Psychiatry, 5*, 179. https://doi.org/10.3389/fpsyt.2014.00179

Xu, Q., Hu, J., Qin, Y., Li, G., Zhang, X., & Li, P. (2023). Intention affects fairness processing: Evidence from behavior and representational similarity analysis of event-related potential signals. *Human Brain Mapping, 44*(6), 2451–2464. https://doi.org/10.1002/hbm.26223

Yanagisawa, K., Nakai, R., Asano, K., Kashima, E. S., Sugiura, H., & Abe, N. (2025). Optimistic people are all alike: Shared neural representations supporting episodic future thinking among optimistic individuals. *Proceedings of the National Academy of Sciences, 122*(30), Article e2511101122. https://doi.org/10.1073/pnas.2511101122

Yoon, L., Somerville, L. H., & Kim, H. (2018). Development of MPFC function mediates shifts in self-protective behavior provoked by social feedback. *Nature Communications, 9*(1), 3086. https://doi.org/10.1038/s41467-018-05553-2

Zhang, X., Zhang, N., Lin, J., Lin, W., He, Z., & Li, H. (2025). Neural and behavioral signatures of feedback-based adjustment bias in response to infant cries. *Neuropsychologia, 218*, Article 109253. https://doi.org/10.1016/j.neuropsychologia.2025.109253